

Chattering Cells: Superficial Pyramidal Neurons Contributing to the Generation of Synchronous Oscillations in the Visual Cortex

Charles M. Gray and David A. McCormick

In response to visual stimulation, a subset of neurons in the striate and prestriate cortex displays synchronous rhythmic firing in the gamma frequency band (20 to 70 hertz). This finding has raised two fundamental questions: What is the functional significance of synchronous gamma-band activity and how is it generated? This report addresses the second of these two questions. By means of intracellular recording and staining of single cells in the cat striate cortex *in vivo*, a biophysically distinct class of pyramidal neuron termed "chattering cells" is described. These neurons are located in the superficial layers of the cortex, intrinsically generate 20- to 70-hertz repetitive burst firing in response to suprathreshold depolarizing current injection, and exhibit pronounced oscillations in membrane potential during visual stimulation that are largely absent during periods of spontaneous activity. These properties suggest that chattering cells may make a substantial intracortical contribution to the generation of synchronous cortical oscillations and thus participate in the recruitment of large populations of cells into synchronously firing assemblies.

In striate and extrastriate areas of the visual cortex of cats and monkeys, many cells display synchronized firing in response to visual stimulation (1). Although the functional significance of this response synchronization is not entirely known, it has been postulated that it contributes to the integration of common visual features in an image (1, 2). It has recently been demonstrated that synchronized firing between cells in different functional columns is often associated with rhythmic discharge in the gamma frequency band (20 to 70 Hz) (3, 4). This finding suggests a functional link between gamma-band oscillations and response synchronization. A prominent feature of gamma-band activity in the visual cortex is the occurrence of repetitive, high-frequency burst discharges in single cells that occurs synchronously with local field potential oscillations (4–7). These bursts of two to five spikes, having intraburst firing rates as high as 800 spikes per second, recur at intervals of approximately 15 to 50 ms (6, 7). Because this pattern of cortical activity is strikingly different from those previously demonstrated to result from intrinsic membrane properties (8), we conjectured that it may represent a class of cells with distinct biophysical properties (9).

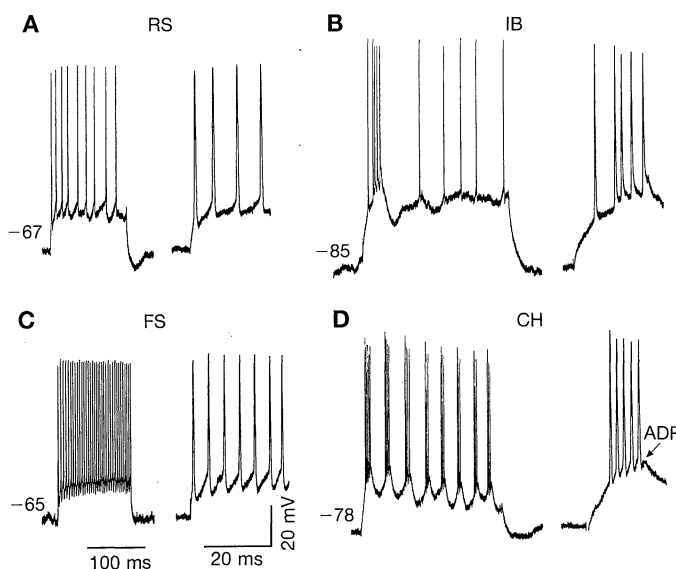
To test this hypothesis, we performed intracellular recording and staining of single cells *in vivo* from the striate cortex of anesthetized cats (10). Our aim was to char-

acterize each cell's intrinsic membrane properties and to determine if these properties bore any relation to the cell's receptive field properties, temporal response properties, morphology, or laminar position. Once a stable intracellular recording was obtained with a resting membrane potential negative to -60 mV, more than 20 megohms input resistance, and overshooting action potentials, we applied hyperpolarizing and depolarizing current pulses (120 to 500 ms at 0.5 Hz) over a range of magnitudes to determine the cell's intrinsic membrane characteristics. In many recordings, we also deter-

mined the cell's orientation and direction selectivity and the location of ON and OFF receptive field subregions and ocular dominance, and then activated the cell with 20 to 30 presentations of an optimal drifting light bar or square wave grating through the dominant eye. At the end of this protocol, the cells were filled with biocytin by injection of 1 nA of hyperpolarizing current, combined with 0.5-nA hyperpolarizing pulses (for 500 ms at 1 Hz), for at least 10 min (11).

The intracellular injection of current into 73 cells from 21 cats revealed four distinct cell classes (Fig. 1). Regular spiking (RS) cells (Fig. 1A; $n = 30$) generated repetitive action potentials that often exhibited spike frequency adaptation in response to current injection. The action potentials of these cells ranged in duration from relatively thin to broad (0.36 to 1.1 ms at half amplitude; mean = 0.62 ± 0.17 ms) and rarely occurred in bursts. Intrinsic bursting (IB) cells (Fig. 1B; $n = 11$) typically displayed an initial burst of two to six spikes superimposed on a slow depolarizing potential, followed by an afterhyperpolarization (AHP) and a transition to tonic firing. The action potentials of these cells were between 0.39 and 0.78 ms in duration (mean = 0.57 ± 0.14 ms) and only rarely did these cells generate repetitive bursts. When repetitive bursting did occur, it did not exceed a frequency of approximately 15 Hz. Fast spiking (FS) cells (Fig. 1C; $n = 7$) displayed tonic firing, at rates as high as 800 Hz, without spike frequency adaptation in response to current pulses that were less than 1.5 nA in amplitude. The action po-

Fig. 1. Responses of the four cell classes to intracellular depolarizing current injection. The initial phase of the response is displayed on a faster time scale to the right. (A) RS pyramidal cell in layer VI. (B) IB pyramidal cell in layer V. (C) FS cell. (D) CH cell in layer III. Note the switch from burst to tonic firing with depolarization in the IB neuron (B), the high-frequency train of action potentials in the FS neuron (C), and the repetitive burst discharges in the CH neuron (D). Action potentials in the CH neuron are associated with the generation of an ADP. The current intensities were 0.6 nA for the RS and FS cells and 0.9 nA for the IB and CH cells. The RS, IB, and CH neurons were all recorded and labeled in the same animal. The data presented in Figs. 2 through 5 are from different cells recorded in six different animals. The data for this and additional figures are available at <http://info.med.yale.edu/neurobio/mccormick/mccormick>.



C. M. Gray, Center for Neuroscience, Section of Neurobiology, Physiology, and Behavior, University of California, Davis, CA 95616, USA. E-mail: cmgray@ucdavis.edu
David A. McCormick, Section of Neurobiology, Yale University School of Medicine, 333 Cedar Street, New Haven, CT 06510, USA. E-mail: david.mccormick@yale.edu

tentials of these cells were very brief in duration (0.16 to 0.48 ms; mean = 0.29 ± 0.09 ms) and they often displayed a pronounced fast AHP. All three of these categories have been previously characterized electrophysiologically in vitro and in vivo (8).

Chattering (CH) cells ($n = 25$) displayed intrinsic firing properties that were markedly different from each of the three

other categories (Figs. 1D and 2). In response to a suprathreshold depolarizing current pulse, these cells displayed repetitive burst discharges of two to five spikes per burst, having an intraburst firing rate as high as 800 spikes per second, and an interburst interval typically ranging from 15 to 50 ms (12). The latency of the first burst in a sequence decreased, and the burst rate and number of spikes per burst increased

with increasing depolarization (Fig. 2, A, B, and D), demonstrating that the bursts are generated by mechanisms intrinsic to the cell. The action potential durations of CH cells (0.14 to 0.58 ms; mean = 0.31 ± 0.12 ms) were similar to those of FS cells, and they exhibited three distinct forms of afterpotentials. After each spike, CH cells displayed a fast AHP that was less than 1 ms in duration and up to 10 mV in amplitude.

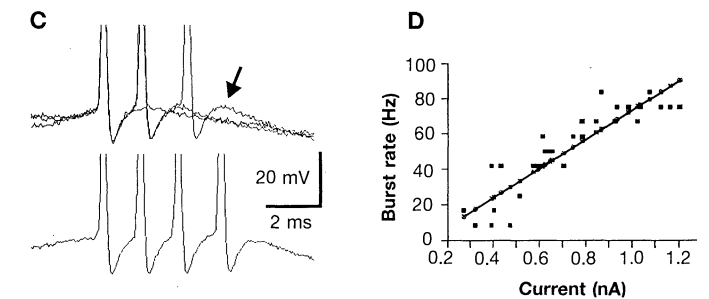
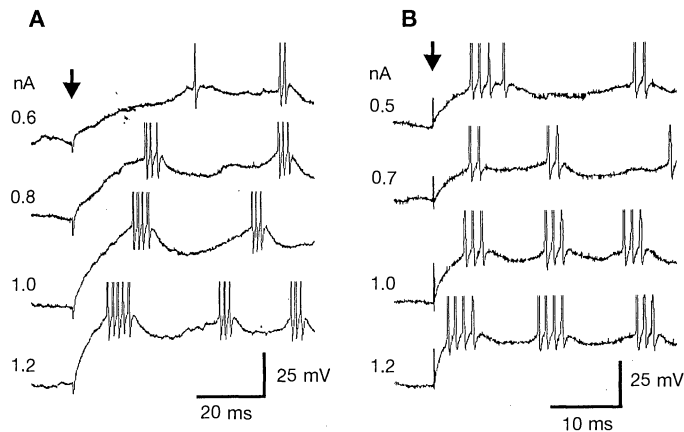


Fig. 2. Repetitive burst firing is an intrinsic property of CH cells. (A) and (B) show the responses of two different CH cells to four different levels of depolarizing current. The beginnings of the current pulses are indicated by arrows. In both cells, the latency of the first burst decreases and the burst rate increases with the level of depolarization. (C) The upper trace shows three superimposed waveforms of one, two, and three action potentials occurring during a burst. The action potentials are very brief and are followed by a rapid AHP and then an ADP (arrow). The second, third, and fourth action potentials of each burst occur during the peak of the ADP of the preceding spike. (D) Scatter plot of bursting rate versus depolarizing current for the cell shown in (B). Each point represents the mean burst rate for each depolarizing current pulse ($n = 104$). The burst rate was proportional to the magnitude of depolarizing current. The linear correlation coefficient is 0.773 ($P \ll 0.0001$).

in the CH cell shown in (A). The lower trace shows a four-spike burst in the same cell. The action potentials are very brief and are followed by a rapid AHP and then an ADP (arrow). The second, third, and fourth action potentials of each burst occur during the peak of the ADP of the preceding spike. (D) Scatter plot of bursting rate versus depolarizing current for the cell shown in (B). Each point represents the mean burst rate for each depolarizing current pulse ($n = 104$). The burst rate was proportional to the magnitude of depolarizing current. The linear correlation coefficient is 0.773 ($P \ll 0.0001$).

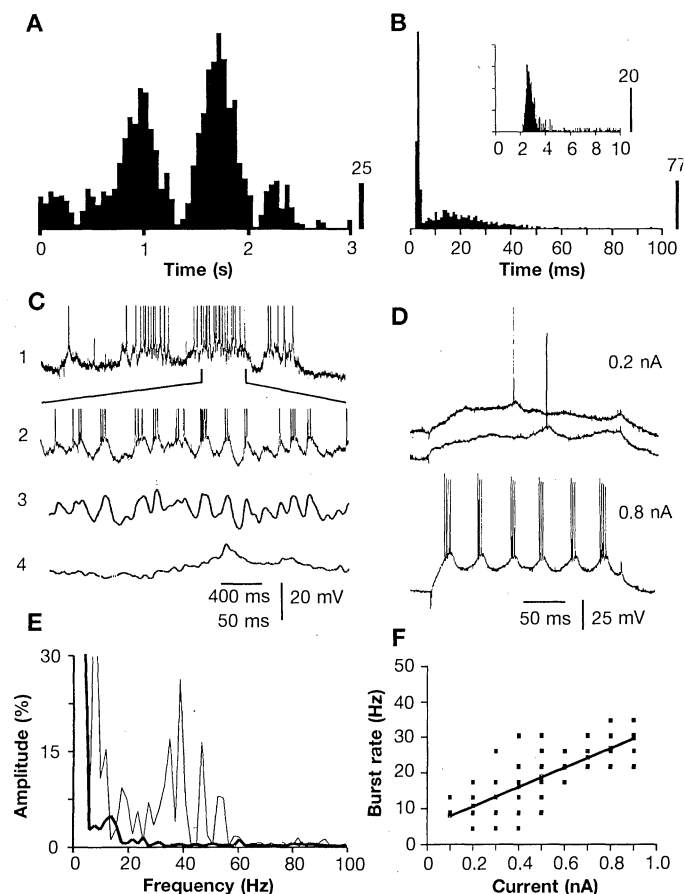


Fig. 3. Activity recorded from a CH cell in response to an optimal visual stimulus (A, B, C, and E) and different levels of intracellular depolarizing current pulses (D and F). The cell had a simple receptive field, belonged to ocular dominance class 4, and was orientation- but not direction-selective. (A) Peristimulus-time histogram (PSTH) recorded in response to 20 presentations of an optimally oriented drifting light bar presented to the contralateral eye. (B) The interspike interval histogram (ISI) computed from the spike trains sampled during the visual response. The characteristic bimodal shape of the distribution reflects the intervals occurring within and between bursts. The inset shows the distribution of intervals less than 10 ms in duration. The peak occurs at approximately 2.5 ms, which indicates that this cell fires at an approximate average of 400 Hz during a burst. (C) Membrane potential of the cell recorded during a single presentation of the stimulus (action potentials are truncated). Trace 1 shows the complete 3-s trial. Trace 2 shows an expanded view of the activity during the peak of the visual response. Traces 3 and 4 show the visually evoked and spontaneous activity, respectively, after removal of the action potentials by the median filter. The oscillations of membrane potential present during the visual response are largely absent in the spontaneous activity. (D) Responses of the cell to two different levels of depolarizing current pulses. The cell shows no evidence of membrane potential oscillations when depolarized near the firing threshold (upper two traces). When the current intensity is increased to depolarize the cell well beyond the firing threshold, a pronounced membrane potential oscillation is evoked that has a frequency near 30 Hz. (E) Fourier power spectra of the median filtered membrane potential shown in traces 3 and 4 of (C). The thick and thin lines represent the spontaneous and stimulus-driven activity, respectively. Frequencies below 10 Hz are truncated. There is a large increase in the amplitude of frequency components between 5 and 10 Hz and between 30 and 60 Hz during the visual response. (F) Scatter plot of bursting rate versus depolarizing current for responses similar to those shown in (D). Each point represents the mean burst rate for each depolarizing current pulse ($n = 33$). The burst rate was proportional to the magnitude of the depolarizing current. The linear correlation coefficient is 0.895 ($P \ll 0.0001$). The responses to current pulses of lower magnitude (0.1 to 0.2 nA) varied between irregular low-frequency bursting and single-spike activity (D).

This was followed by a small (2 to 5 mV) afterdepolarization (ADP) that could trigger an additional action potential (Fig. 2C), which suggests that this event is critical to the generation of bursts. A pronounced AHP, having an amplitude of 5 to 15 mV and a duration of 10 to 40 ms, followed each burst. During sustained depolarization, this slow AHP gave rise to regular, repetitive burst discharges, a pattern that never occurred in response to brief (10 to 20 ms) depolarizing pulses. In individual CH cells, the burst frequency occurred within a limited range (see Fig. 2D and Fig. 3F), although as a group, CH cells could oscillate at frequencies ranging from 20 to 80 Hz. CH cells often displayed a mixture of periodic and nonperiodic firing patterns, particularly at low current intensities, that could be influenced by the background synaptic activity. These cells also showed no evidence of membrane potential oscillations in the 20- to 70-Hz range when activated by subthreshold currents.

In addition to these characteristics, the visual response properties of CH cells clearly distinguished them from the other three cell classes. An example of the activity recorded from one CH cell is shown in Fig. 3. A dominant property of these cells was their tendency to fire in repetitive bursts of action potentials at rates of 20 to 70 Hz in response to optimal visual stimuli (Fig. 3C; $n = 16$). This property led to a characteristic bimodal shape of their interspike interval histograms, with a large percentage of intervals occurring at durations of 1 to 3 ms (inset, Fig. 3B). Similar to their responses to depolarizing current pulses, CH cells displayed a marked post-burst membrane repolarization of 5 to 15 mV that resulted in a pronounced but transient period of inhibition of firing between bursts (Fig. 3C). These large rhythmic fluctuations of membrane potential occurred only during the response to visual stimuli. We quantified their properties by removing the action potentials with a median filter and then computing the Fourier power spectrum of the membrane potential during periods of spontaneous and visually evoked activity. As shown in Fig. 3, C and E, the membrane potential during the visual response of this cell was dominated by frequencies in the range of 30 to 60 Hz. In all of the CH cells, the frequency distribution varied from trial to trial, and the rhythmic fluctuations showed no evidence of being locked to the stimulus presentation (Fig. 4). The gamma-band oscillations were largely absent during periods of spontaneous activity (13) and exhibited frequency distributions similar to those previously reported for the extracellular field potential during visual stimulation (5).

Using both the intrinsic and visual response properties as criteria, we subjectively classified each cell as belonging to one of the four classes: RS, IB, FS and CH. We then applied three quantitative measures to the visual responses recorded from a subset of cells ($n = 28$): the mean firing rate during the peak of the visual response, the percentage of interspike intervals less than 3 ms in duration, and the cumulative spectral power of the membrane potential in the range of 25 to 65 Hz (14). Although there was a wide range of response magnitudes, CH cells consistently fired at higher rates than did the other three classes of cells, whereas IB cells discharged at the lowest rates (15). Our sample of two visually responsive FS cells was insufficient to make a valid comparison for this cell group. With respect to their interspike interval distributions, CH cells displayed the greatest propensity for burst firing at high intraburst firing rates and could be distinguished from the other three cell classes on the basis of this measure alone (16). Although IB cells also fired in bursts during a visual response,

the number of bursts in each response and the intraburst firing rate were much smaller than those of CH cells (17). With respect to membrane potential fluctuations, CH cells exhibited larger gamma-band oscillations during the response to visual stimuli as compared with the other three cell classes [CH > RS ($P \ll 0.0001$), CH > IB ($P \ll 0.0001$), and CH > FS ($P \ll 0.0001$); Kolmogorov-Smirnov test]. Moreover, the visually evoked oscillations in CH cells were greater than those recorded in the absence of visual stimulation ($P \ll 0.0001$) (17). Figure 4 shows representative examples of the membrane potential recorded on separate trials in a CH cell and an RS neuron. The stimulus-evoked fluctuations contain multiple frequencies in the range of 20 to 70 Hz, and the frequency distribution varies widely from trial to trial.

In addition to their intrinsic response properties, we were able to determine the receptive field properties of a subset of the RS, IB, and CH cells. Of the cells unambiguously classified ($n = 21$), all of the RS ($n = 10$) and CH cells ($n = 7$) had simple recep-

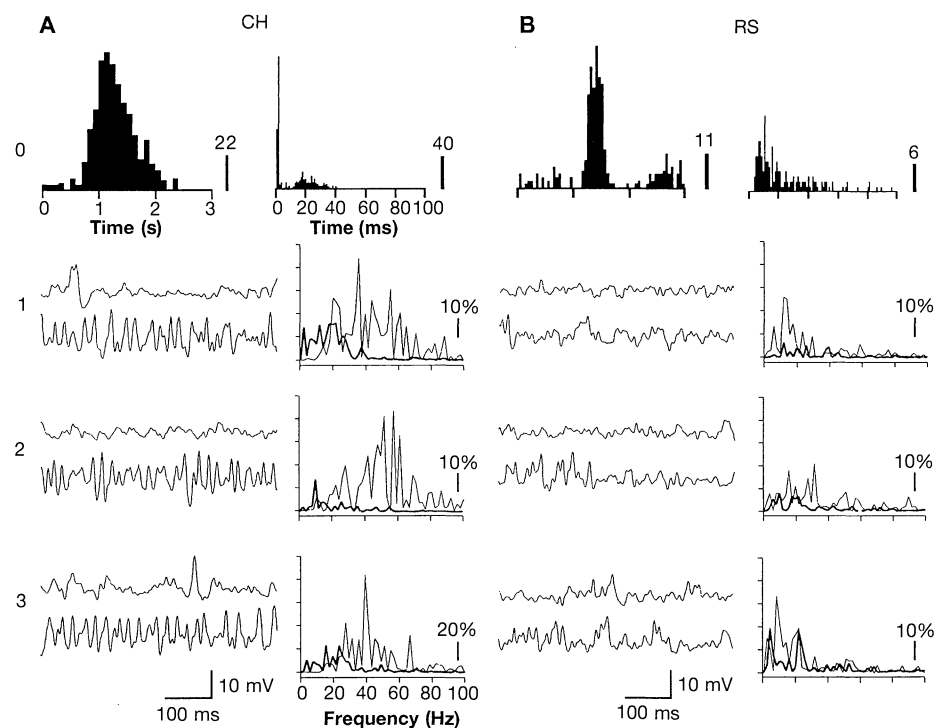


Fig. 4. Examples of spontaneous and visually evoked membrane potential fluctuations in a CH cell (A) and an RS neuron (B). The upper left and right plots in (A) and (B) show the PSTH and the ISIH, respectively. The CH cell has a characteristic bimodal ISIH, whereas the RS neuron has a longer refractory period and a unimodal distribution of intervals. The lower three rows in (A) and (B) show three examples of the membrane potential recorded in three separate trials before (upper plot) and during (lower plot) the response to an optimal visual stimulus. The corresponding power spectra for each epoch are shown to the right of each pair of membrane potential traces. The thick and thin lines represent the spontaneous and visually driven activity, respectively. The raw data were median-filtered to remove the spikes and then bandpass-filtered (at 10 to 100 Hz). The spectral plots were normalized to the peak value across the 12 spectra, and the amplitude was expressed as a percentage of that value. Consistent with the cumulative results, the CH cell displays large gamma-band fluctuations in membrane potential during the visual responses that are largely absent or much smaller in magnitude in the RS neuron.

tive fields, whereas all of the IB cells ($n = 4$) had complex receptive fields. Of the latter, three clearly fell into the category of standard complex on the basis of their responses to drifting bars of varying length (18).

We recovered the morphology and laminar position of 24 neurons. RS cells were found to be pyramidal neurons in both the supra- and infragranular layers ($n = 8$), as reported previously (8). Two IB cells were labeled, and these were large, layer V, spiny pyramidal neurons with apical dendrites extending up to layer I. All of the FS neurons that were recovered ($n = 3$) were found to be aspiny basket cells located in the super-

ficial laminae. Strikingly, all 11 of the CH cells recovered were located in layers II and III. Seven of these cells were labeled well enough that their complete dendritic arbors and the path of their main axon could be examined. All seven cells possessed an axon that extended into the white matter, apical dendrites extending into layers I and II, and dendritic processes that were moderately to densely covered with spines (Fig. 5). All seven cells appeared as typical layer II/III pyramidal neurons except for one. This CH cell possessed a round cell body and multiple spiny dendritic processes, including one that extended toward layer I

and an axon extending into the white matter, which suggests that it was a modified pyramidal cell. Three of the CH cells were labeled well enough that their axon collaterals could be followed some distance from the cell soma. In these cells, the axon branched and sent collaterals in layers I, II, III, and V. Figure 5 shows an example of one of these CH cells. The dendrites are densely covered with spines and the axon extends within the local region of the dendritic arbor, as well as horizontally in layers II, III, and V, and into the white matter.

Contrary to earlier observations (13, 19), these data demonstrate that a previously uncharacterized class of cells, which are likely to be excitatory, are pyramidal in morphology, have simple receptive field properties, are located in supragranular layers, and have corticocortical axonal projections, are capable of intrinsically generating repetitive burst discharges at 20 to 70 Hz in response to depolarization (20). The conductance mechanisms controlling the repetitive bursting require suprathreshold activation because no evidence was found for subthreshold oscillations in these cells. These findings suggest that a major component of visually evoked cortical gamma-band oscillations may be controlled by the intrinsic membrane properties and axonal interconnections of CH cells, and hence be due to an intracortical mechanism (21). Cells that receive presynaptic input from CH cells would therefore be expected to display membrane potential oscillations having properties consistent with a synaptic rather than an intrinsic mechanism (13). Of course, if CH cells were synaptically connected to one another, the oscillatory activity in these cells would reflect both mechanisms. In our own preliminary observations, CH cells do receive rhythmic 30- to 70-Hz barrages of postsynaptic potentials during the presentation of visual stimuli. The finding that synchronization is often associated with the presence of repetitive bursts of action potentials that are identical to those generated by CH cells (3, 4, 5) suggests that these cells may play an important, if not crucial, role in the generation of long-range response synchronization in the visual cortex.

Several of the properties of CH cells may facilitate their participation in the generation of visually driven synchronous activity in the cortex. Experimental and theoretical studies suggest that bursts of action potentials may provide a particularly effective form of presynaptic input onto a cortical neuron. The rapid firing within a burst can lead to temporal summation postsynaptically (22) and can dramatically increase the probability of neurotransmitter release from the presynaptic neuron (22, 23). The large

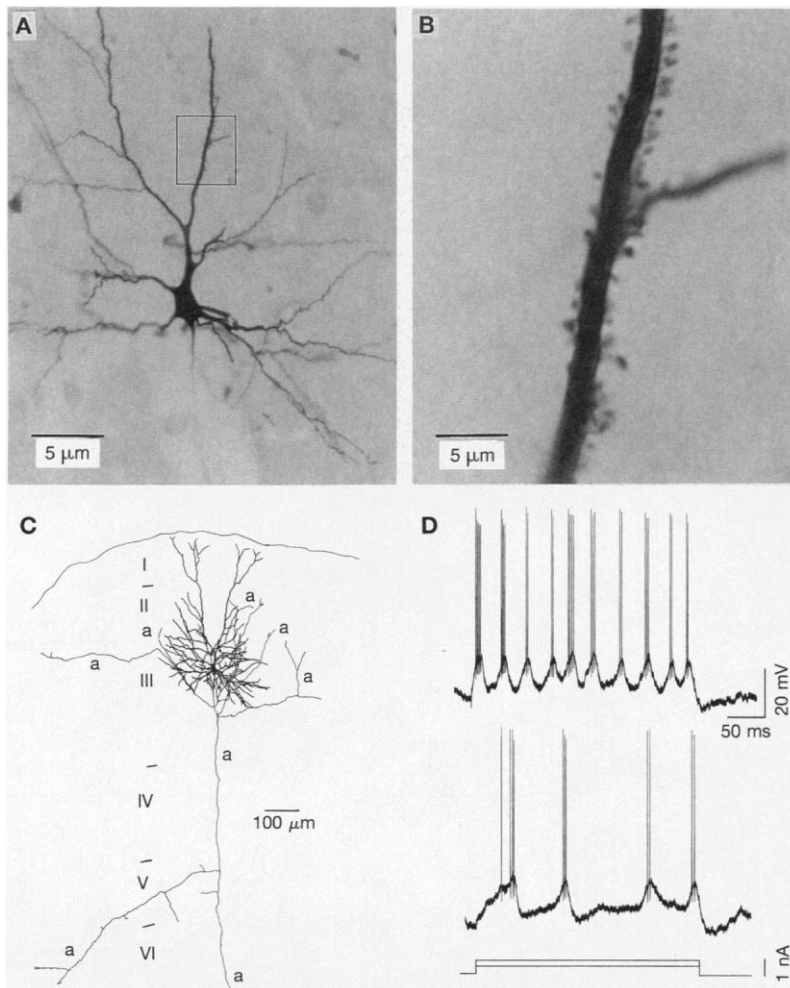


Fig. 5. Example of a labeled CH cell having spiny pyramidal morphology, with its soma located in layer III. **(A)** Low-power light field micrograph showing that the filled cell has morphological features that are characteristic of superficial pyramidal neurons. **(B)** High-power micrograph of apical dendritic region outlined by the rectangle in **(A)**. There is a high density of dendritic spines. **(C)** Camera lucida reconstruction of the cell. The dendrites and axon are indicated by the thick and thin lines, respectively. The cortical layers are indicated by the roman numerals I through VI. The axon branches and sends out collaterals in layers II, III, and V. Local axon collaterals are indicated by the letter a. The axon also projects into the white matter (not shown). **(D)** Responses of the cell to two different levels of intracellular depolarizing current pulses. In both traces, the cell exhibits high-frequency bursts of action potentials that are characteristic of CH cells. The pattern of burst firing is rhythmic when the cell is depolarized strongly. At lower levels of depolarization, the cell continues to burst, but in a temporally disorganized manner. There is no apparent evidence of an underlying subthreshold membrane potential oscillation in the lower trace.

AHP that follows a burst of spikes may produce brief periods of decreased excitability, causing synaptic inputs out of phase with the oscillation to be rejected. Finally, our preliminary studies indicate that CH cells have axon collaterals that extend horizontally and ramify within layers I, II, III, and V, in addition to projecting out of the local cortical region, as has been reported previously for layer II/III pyramidal cells (24). These findings place CH cells in a key position, both biophysically and anatomically, for the generation of synchronous cortical activity (25). The postsynaptic targets of these cells, the mechanisms for generation of "chattering," and the functional consequences of synchronous repetitive burst firing are important topics that remain to be explored.

REFERENCES AND NOTES

1. W. Singer and C. M. Gray, *Annu. Rev. Neurosci.* **18**, 555 (1995).
2. P. Milner, *Psychol. Rev.* **81**, 521 (1974); C. von der Malsburg, Internal Report, Max-Planck-Institute for Biophysical Chemistry, Göttingen, West Germany (1981); *Ber. Bunsen-Ges. Phys. Chem.* **89**, 703 (1985); C. von der Malsburg and W. Schneider, *Biol. Cybern.* **54**, 29 (1986); W. Singer, *Annu. Rev. Physiol.* **55**, 349 (1993).
3. A. Frien, R. Eckhorn, R. Bauer, T. Woelbern, H. Kehr, *Neuroreport* **5**, 2273 (1994); P. Koenig, A. K. Engel, W. Singer, *Proc. Natl. Acad. Sci. U.S.A.* **92**, 290 (1995); S. R. Friedman-Hill, P. E. Maldonado, C. M. Gray, *Soc. Neurosci. Abstr.* **21**, 592.3 (1995).
4. M. Livingstone, *J. Neurophysiol.* **75**, 2467 (1996).
5. C. M. Gray and W. Singer, *Soc. Neurosci. Abstr.* **13**, 404.3 (1987); R. Eckhorn *et al.*, *Biol. Cybern.* **60**, 121 (1988); C. M. Gray and W. Singer, *Proc. Natl. Acad. Sci. U.S.A.* **86**, 1698 (1989); A. K. Engel, P. König, C. M. Gray, W. Singer, *Eur. J. Neurosci.* **2**, 588 (1990).
6. D. H. Hubel and T. N. Wiesel, *J. Neurophysiol.* **28**, 229 (1965); C. M. Gray, A. K. Engel, P. König, W. Singer, *Eur. J. Neurosci.* **2**, 607 (1990).
7. C. M. Gray and G. Viana Di Prisco, *Soc. Neurosci. Abstr.* **19**, 359.8 (1993); C. M. Gray, S. R. Friedman-Hill, P. E. Maldonado, *ibid.* **21**, 592.2 (1995).
8. B. W. Connors, M. J. Gutnick, D. A. Prince, *J. Neurophysiol.* **48**, 1302 (1982); D. A. McCormick, B. W. Connors, J. W. Lighthall, D. A. Prince, *ibid.* **54**, 782 (1985); A. Larkman and A. Mason, *J. Neurosci.* **10**, 1407 (1990); A. Mason and A. Larkman, *ibid.*, p. 1415; A. Nunez, F. Amzica, M. Steriade, *J. Neurophysiol.* **70**, 418 (1993).
9. D. A. McCormick, C. M. Gray, Z. Wang, *Soc. Neurosci. Abstr.* **19**, 359.9 (1993); D. A. McCormick and C. M. Gray, *ibid.* **21**, 592.6 (1995).
10. Each cat was anesthetized with an intramuscular injection of ketamine (12 to 15 mg per kilogram of body weight) and xylazine (1 mg/kg) and given atropine (0.05 mg/kg) to reduce salivation. A continuous infusion of Ringer solution containing 2.5% dextrose was given intravenously (i.v.) throughout the experiment (4 ml/kg per hour). Anesthesia was maintained throughout with halothane (0.6 to 1.2%), in a mixture of nitrous oxide and oxygen (2:1), while the animals were actively ventilated with a respirator pump. The electrocardiogram, heart rate, rectal body temperature, and expiratory CO₂ concentration were continuously monitored, and the latter three were maintained within the ranges of 140 to 180 beats per minute, 37.5° to 39.0°C, and 3.5 to 4.5%, respectively. Each animal was mounted in a stereotaxic frame, and in order to minimize pulsations arising from the heartbeat and respiration, the cisterna magna was cannulated, a bilateral pneumothorax was performed, and the animal was suspended from the stereotaxic frame. A craniotomy (3 to 4 mm) was made overlying the representation of the area centralis of area 17. After the surgery, the animals were paralyzed with pancuronium bromide (3 mg/kg), followed by a continuous infusion of 3 mg/kg per hour (i.v.). The eyes were focused on the screen of a computer monitor at a distance of 57 cm by means of an appropriate pair of gas-permeable contact lenses. The nictitating membranes were retracted and the pupils were dilated by local application of phenylephrine and atropine, respectively. A small opening was made in the dura, and a micropipette was positioned just above the cortical surface. A 4% mixture of agar in Ringer solution was applied to the cortical surface to reduce pulsations. Within 10 to 12 hours of recording and staining of the first cell, each animal was given a lethal injection of nembutal and perfused through the heart with phosphate-buffered saline (PBS), followed by PBS containing 2% paraformaldehyde and 1.25% glutaraldehyde. This protocol was approved by the University of California, Davis, and Yale University Institutional Animal Care and Use Committees and conforms to the guidelines recommended in *Preparation and Maintenance of Higher Mammals During Neuroscience Experiments*, NIH publication No. 91-3207 (National Institutes of Health, Bethesda, MD, 1991).
11. Intracellular recordings were obtained with the use of conventional "sharp" electrodes, pulled on a Flaming-Brown P87-PC pipette puller, filled with 1.5 M K⁺-acetate and 2% biocytin, and beveled to a final resistance of 70 to 120 megohms. After each recording, the depth of the electrode tip was noted and the position of the recording site was marked on the skull. A new site was chosen at least 1 mm away from any previous recording site and the entire procedure was repeated. Visual stimuli were generated by a personal computer and displayed on a 19-inch color monitor (80-Hz noninterlaced refresh rate; 1024 × 768 resolution). The data were digitized at a rate of 20 kHz and processed offline. For each cell, we computed the peristimulus-time histogram (PSTH), the autocorrelation histogram (ACH), the power spectrum of the ACH, the interspike interval histogram (ISIH), and the power spectrum of the membrane potential fluctuations occurring spontaneously and in response to visual stimulation. For histology, a block of tissue containing the filled cells was sunk in 30% sucrose. Coronal sections 60 to 75 μm thick were made and were reacted for the presence of biocytin, with the use of standard techniques and diaminobenzidine visualization. The histological sections were cover-slipped and examined for the presence of labeled cells. Filled neurons were photographed and reconstructed with a camera lucida.
12. Surprisingly, intrinsic firing patterns similar to those displayed by CH cells have rarely been observed in cortical *in vitro* slice preparations (8) [Y. Kang and F. Kayano, *J. Neurophysiol.* **72**, 578 (1994)]. This raises the issue that cellular damage may account for the behavior of CH cells. We believe this interpretation to be highly unlikely for at least four reasons. First, using extracellular single-unit recordings in area 17 in both alert (7) and anesthetized (4, 6) cats and monkeys, we and others have observed a substantial number of cells having temporal firing characteristics virtually identical to those reported here for CH cells. Second, the consistency of the receptive field properties, morphology, and laminar positions of the CH cells indicate that they belong to a distinct category of cells. Third, we have observed CH cells in slices of the cat visual cortex *in vitro*, and the probability of finding these cells is greatly enhanced by the application of a muscarinic cholinergic agonist such as acetyl-β-methylcholine (26). This raises the possibility that neuromodulatory transmitters such as acetylcholine, which may be dramatically reduced in the slice, can modify the intrinsic properties of CH cells. This interpretation is also consistent with the recent observation that stimulation of the mesencephalic reticular formation enhances the occurrence and magnitude of synchronous cortical oscillations in the gamma frequency band (27). Fourth, injury, or the decay of recording quality, did not induce any of the "non-CH" cells to become CH neurons.
13. B. Jagadeesh, C. M. Gray, D. Ferster, *Science* **257**, 552 (1992); V. Bringuier, Y. Fregnac, D. Debanne, D. Shulz, A. Baranyi, *Neuroreport* **3**, 1065 (1992).
14. We selected a sample of 28 visually responsive cells that we recorded long enough to collect at least 20 responses to the presentation of an optimally oriented drifting light bar. The spike trains were extracted from each trial and quantified with the use of two measures: the mean firing rate across trials for a 500-ms epoch centered on the peak of the visual response and the percentage of interspike intervals occurring during the visual responses that were <3 ms in duration. For the subthreshold membrane potential, we visually selected two 512-ms epochs from each trial, one during the period of spontaneous activity and the other centered on the peak of the visual response. For both epochs on each trial, we applied a seven-point median filter to remove the action potentials and stored the resulting signals at a resolution of 1 ms. The data were digitally filtered (10 to 100 Hz) to remove both low- and high-frequency components. The power spectrum was then computed for each epoch of data. The sum of all values in each spectrum between 25 and 65 Hz was computed and the distributions were compared, after normalization to the largest value in the data set, with the use of the Kolmogorov-Smirnov test.
15. The firing rates (in spikes per second; means ± SD) of the four cell types were as follows: RS ($n = 10$), 26 ± 7 ; IB ($n = 5$), 18 ± 1 ; FS ($n = 2$), 27 ± 1 ; and CH ($n = 11$), 45.4 ± 22 . $RS > IB$ ($P < 0.03$); $CH > RS$ ($P < 0.009$); and $CH > IB$ ($P < 0.002$).
16. The percentages of intervals <3 ms for the four cell types (means ± SD) were as follows: RS ($n = 10$), 0.6 ± 1.2 ; IB ($n = 5$), 1.4 ± 2.1 ; FS ($n = 2$), 3.8 ± 4.6 ; and CH ($n = 11$), 27.5 ± 10.8 . $CH > RS$ ($P < 0.0003$); $CH > IB$ ($P < 0.007$).
17. C. M. Gray and D. A. McCormick, data not shown.
18. L. A. Palmer and A. C. Rosenquist, *Brain Res.* **67**, 27 (1974); C. D. Gilbert, *J. Physiol.* **268**, 391 (1977); P. Hammond and B. Ahmed, *Neuroscience* **15**, 639 (1985).
19. R. R. Llinás, A. A. Grace, Y. Yarom, *Proc. Natl. Acad. Sci. U.S.A.* **88**, 897 (1991).
20. A pattern of repetitive burst firing in fast pyramidal tract cells in layer V has been previously demonstrated by W. H. Calvin and G. W. Syper [Brain Res. **83**, 498 (1975)]. These repetitive bursts exhibited intraburst frequencies of 400 to 500 Hz and interburst frequencies of 80 to 90 Hz, and occurred only with strong depolarization.
21. M. Lauffer and M. Verzeano, *Vision Res.* **7**, 215 (1967); G. M. Ghose and R. D. Freeman, *J. Neurophysiol.* **68**, 1558 (1992); S. Neunenschwander and W. Singer, *Nature* **379**, 728 (1996).
22. R. Miles and R. K. S. Wong, *J. Physiol.* **373**, 397 (1986); A. M. Thomson, J. Deuchars, D. C. West, *Neuroscience* **54**, 347 (1993).
23. C. F. Stevens and Y. Wang, *Neuron* **14**, 795 (1995).
24. C. D. Gilbert and T. N. Wiesel, *J. Neurosci.* **3**, 1116 (1983); K.A. Martin and D. Whitteridge, *J. Physiol. (London)* **353**, 463 (1984).
25. Synchronous gamma-band activity is prevalent in the hippocampus of behaving rats [A. Bragin *et al.*, *J. Neurosci.* **15**, 47 (1995)] and can also be recorded in the hippocampal and neocortical slice preparations [M. A. Whittington, R. D. Traub, J. G. R. Jefferys, *Nature* **373**, 612 (1995)]. In the hippocampal slice, gamma-band activity appears to be generated by networks of inhibitory interneurons [R. D. Traub, M. A. Whittington, S. B. Colling, G. Buzsáki, J. G. R. Jefferys, *J. Physiol.* **493**, 471 (1996)]. These data suggest that the cellular mechanisms generating gamma-band activity may be different for the hippocampus and visual cortex.
26. D. A. McCormick and L. Nowak, *Soc. Neurosci. Abstr.*, in press.
27. M. Steriade, F. Amzica, D. Contreras, *J. Neurosci.* **16**, 392 (1996); M. H. J. Munk, P. R. Roelfsema, P. König, A. K. Engel, W. Singer, *Science* **272**, 271 (1996).
28. We thank L. Nowak and R. Azouz for their valuable contributions to this work. Supported by a grant from the National Eye Institute and a contract from the Office of Naval Research to C.M.G., and by grants from NIH and NSF to D.M.

7 June 1996; accepted 15 August 1996